

Supporting Information

Quantum Mechanical Calculations of Vibrational Sum-Frequency-Generation (SFG) Spectra of Cellulose: Dependence of the CH and OH Peak Intensity on the Polarity of Cellulose Chains within the SFG Coherence Domain

Christopher M. Lee,^{1†} Xing Chen,^{2†} Philip A. Weiss,² Lasse Jensen,^{2*} and Seong H. Kim^{1*}

1. Department of Chemical Engineering and Materials Research Institute, The Pennsylvania State University, PA, 16802, USA
2. Department of Chemistry, The Pennsylvania State University, PA, 16802, USA

[†]Equally contributed to this work

* Corresponding authors: jensen@chem.psu.edu, shkim@engr.psu.edu

I. Computational details of TD-DFT calculations

The fractional coordinates of unit cell were transformed into Cartesian space using the rotation matrix¹:

$$\begin{bmatrix} x_c \\ y_c \\ z_c \end{bmatrix} = \begin{bmatrix} a & b\cos\gamma & c\cos\beta \\ 0 & b\sin\gamma & c\frac{\cos\alpha - \cos\beta\cos\gamma}{\sin\gamma} \\ 0 & 0 & \frac{v}{abs\gamma} \end{bmatrix} \begin{bmatrix} x_f \\ y_f \\ z_f \end{bmatrix}$$

where a, b, and c are the unit vectors of the unit cell axes; α , β , and γ are the inter-axis angles, and v is the volume of a parallelepiped, which is given by,

$$v = abc\sqrt{1 - \cos^2(a) - \cos^2(b) - \cos^2(c) + 2\cos(a)\cos(b)\cos(c)}$$

Cellulose I α and I β are featured by two chains in the unit cell which includes 2 dimers; each dimer consists of two anhydroglucose monomers. To model intermolecular hydrogen bonding interactions, it is required to translate the monomeric units along the unit cell vectors using a rotation matrix along the a, b, and c unit cell directions:

$$T_a = 1 + [a \ 0 \ 0]$$

$$T_b = 1 + [bcos\gamma \ bsin\gamma \ 0]$$

$$T_c = 1 + \left[ccos\beta \quad c \frac{cos\alpha - cos\beta cos\gamma}{sin\gamma} \quad \frac{\nu}{absin\gamma} \right]$$

To represent the structural character of crystalline, the computational models of cellulose I α and I β are constructed by stacking two units of dimers, as shown in Figure 1.

Under the Born-Oppenheimer approximation and the dipole approximation, the hyperpolarizability is written as a product of the derivatives of dipole and polarizability with respect to mass-weighted normal modes (Q_q):

$$\beta_{abc}(\omega_{SFG}, \omega_{VIS}, \omega_{IR}) = \sum_q \frac{-\hbar}{2\omega_q} \frac{\partial\alpha_{ab}}{\partial Q_q} \frac{\partial\mu_c}{\partial Q_q} \left(\frac{1}{\omega_{IR} - \omega_q + \Gamma_q} \right)$$

The polarizability and dipole were obtained from TD-DFT calculations. Their derivatives were calculated numerically by using three-point differentiation:

$$\frac{\partial\alpha}{\partial Q_q} = \frac{\alpha(Q_q + \Delta Q_q) - \alpha(Q_q - \Delta Q_q)}{2s_Q \Delta Q_q}$$

$$\frac{\partial \mu}{\partial Q_q} = \frac{\mu(Q_q + \Delta Q_q) - \mu(Q_q - \Delta Q_q)}{2s_Q \Delta Q_q}$$

where s_Q is the mass-weighted step size. The polarizability and dipole are calculated at the equilibrium geometry distorted along the normal mode coordinate in the positive and negative direction.

In eq. (2) of the main manuscript which transforms the molecular hyperpolarizability $\beta_{x'y'z'}$, obtained from the Placzek approximation (eq.1) to the second-order susceptibility tensor ($\chi_{XYZ}^{(2)}$), the z-x-z the transformation matrix was used:

$$\langle R_{xx}, R_{yy}, R_{zz} \rangle = \begin{bmatrix} \cos\phi\cos\psi - \sin\phi\cos\theta\sin\psi & -\sin\phi\cos\theta\cos\psi - \cos\phi\sin\psi & \sin\phi\sin\theta \\ \sin\phi\cos\psi + \cos\phi\cos\theta\sin\psi & \cos\phi\cos\theta\cos\psi - \sin\phi\sin\psi & -\cos\phi\sin\theta \\ \sin\theta\sin\psi & \sin\theta\cos\psi & \cos\theta \end{bmatrix}$$

where the angles θ, ϕ, ψ are defined as the polar, azimuth and twist angles, respectively.

The second-order susceptibility for parallel packing is obtained straightforwardly, as the model is placed in the lab frame:

$$\chi_{XYZ(parallel)}^{(2)} = \chi_{XYZ(+)}^{(2)}$$

The second-order susceptibility for antiparallel packing is obtained by rotating the azimuthal angle of one unit by 180° ($\chi_{XYZ(-)}^{(2)}$) and then averaging the susceptibilities of this rotated unit and the original unit:

$$\begin{aligned} \chi_{XYZ(-)}^{(2)} &= C(z)\chi_{XYZ(+)}^{(2)} \\ \chi_{XYZ(antiparallel)}^{(2)} &= \frac{(\chi_{XYZ(+)}^{(2)} + \chi_{XYZ(-)}^{(2)})}{2} \end{aligned}$$

where $C(z)$ is the rotation matrix around the surface normal:

$$C(z) = \begin{bmatrix} \cos\alpha & -\sin\alpha & 0 \\ \sin\alpha & \cos\alpha & 0 \\ 0 & 0 & 1 \end{bmatrix}$$

where α is the azimuthal angle around the surface normal (here, α equals π).

The simulated SFG intensity is proportional to the square of effective second-order susceptibility, as shown in eq. (3) of the main manuscript. For example, in order to obtain the SFG intensity for the parallel-packed cellulose crystallites using a *ssp* polarization combination of the probe pulses (s-polarized SFG signal, *s*-polarized visible beam, and *p*-polarized IR beam), only two terms of $\chi_{eff(parallel)}^{(2)}$ can be used:

$$\chi_{eff,ssp(parallel)}^{(2)} = \chi_{YYZ(parallel)}^{(2)} L_{yy}(\omega_{SFG}) L_{yy}(\omega_{VIS}) L_{zz}(\omega_{IR}) \sin\gamma_{IR} + \chi_{YYX(parallel)}^{(2)} L_{yy}(\omega_{SFG}) L_{yy}(\omega_{VIS}) L_{xx}(\omega_{IR}) \sin\gamma_{IR}$$

where γ_{IR} is the incident angle for the IR beam and $L_{ij}(\omega_{ij})$ are the frequency-dependent Fresnel factors. The SFG intensity for the antiparallel-packed crystallites can be calculated from the term containing $\chi_{YYZ(antiparallel)}^{(2)}$ only, since $\chi_{YYX(antiparallel)}^{(2)}$ is zero for the truncated dimeric model shown in Figure 1. Note that Figures 2 and 3 in the main manuscript were produced without considering the Fresnel factors (so, setting them to be 1). The Fresnel factors vary with the experimental geometry. The expressions for the other seven combinations (*sss*, *pss*, *ppp*, *psp*, *spp*, and *pps*) can be constructed similarly using the method described previously.²

II. TD-DFT calculation results

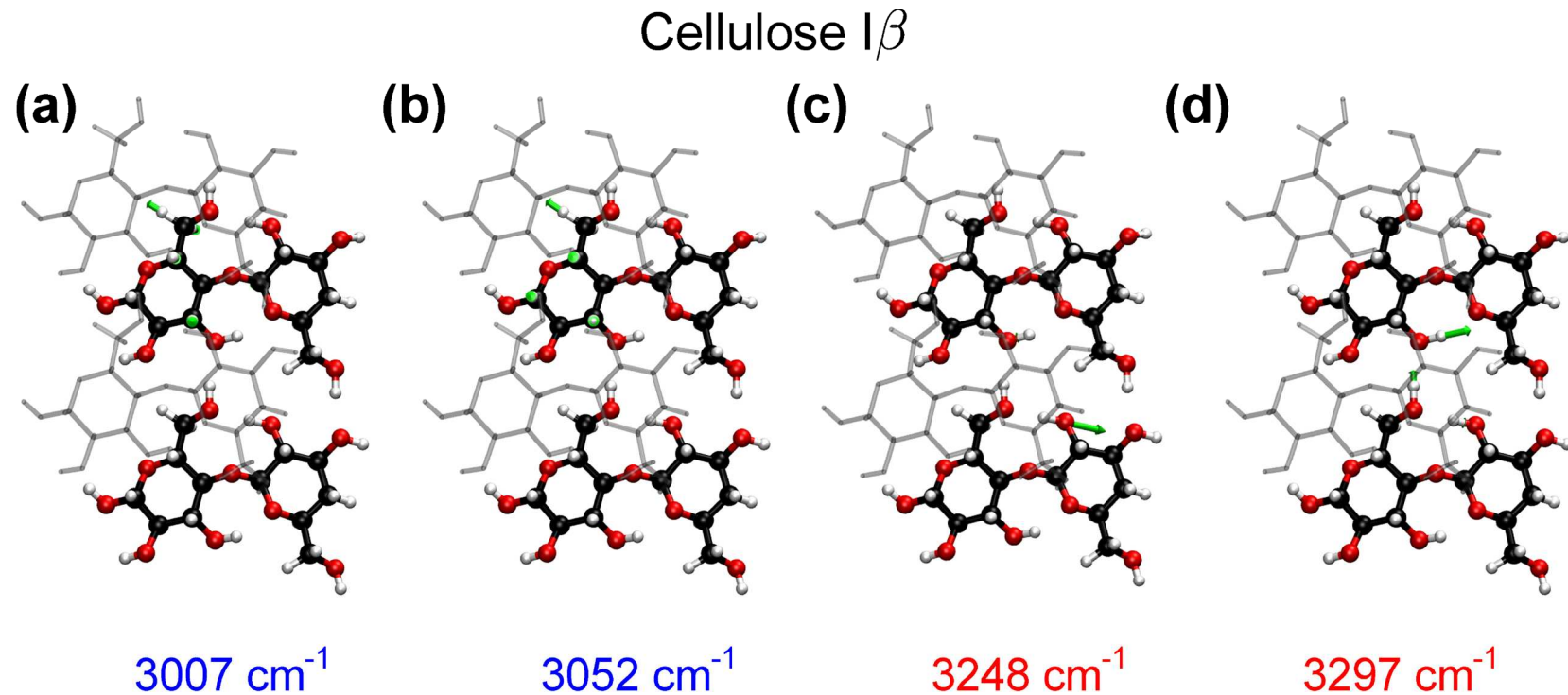


Figure S1. Selected C-H (a, b) and O-H (c, d) normal modes of cellulose I β . The layer involved in the dominant vibrations is in stick and ball and other layer is in transparent representation.

Cellulose I α

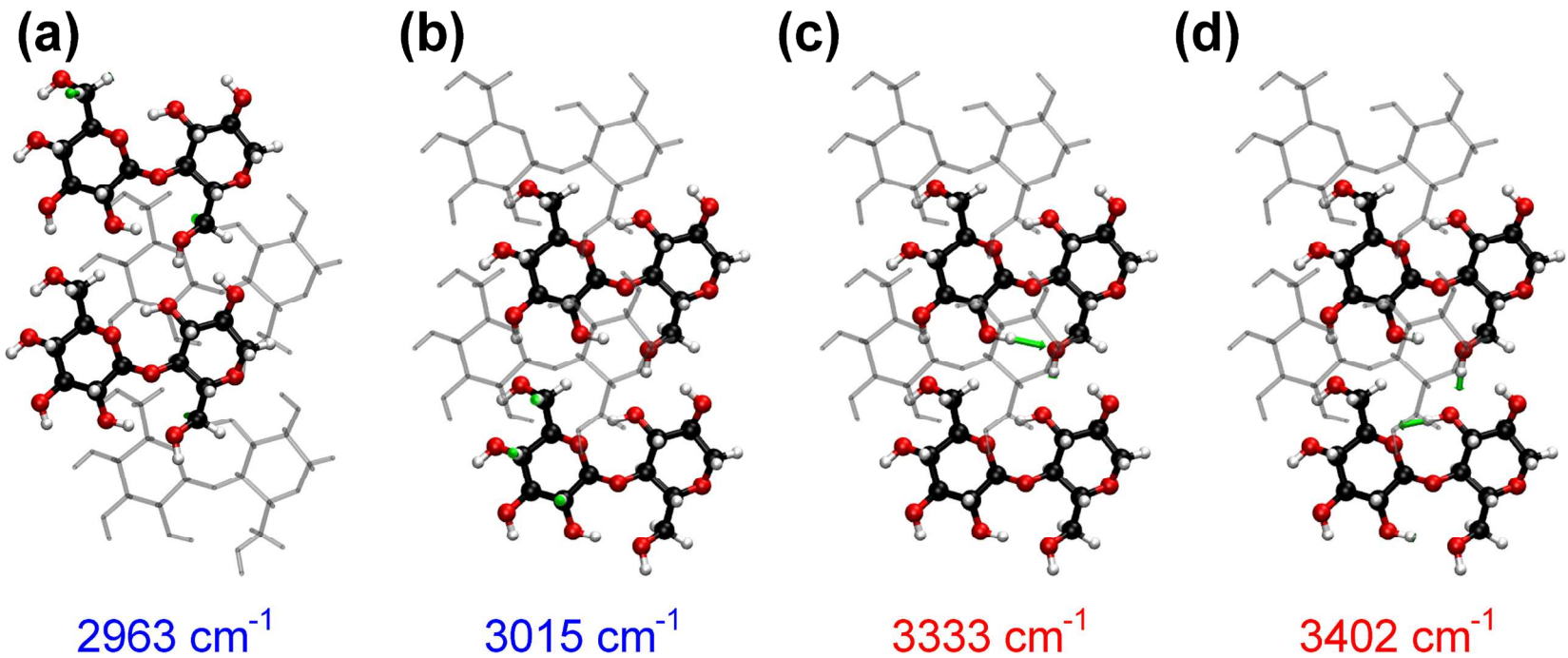


Figure S2. Selected C-H (a, b) and O-H (c, d) normal modes of cellulose I α . The layer involved in the dominant vibrations is in stick and ball and other layer is in transparent representation.

Table S1. Magnitude of second order susceptibility (in the atomic unit, $e^3 a_0^3 / E_h^2$) relevant to *ssp*, *ppp*, and *psp* polarization of cellulose I β parallel. The C-H and O-H normal modes are presented with blue and red, respectively. The rows in gray signify the components contributing to the SFG signal measured with the *ppp* polarization combination.

Parallel	2999 cm ⁻¹	3007 cm ⁻¹	3024 cm ⁻¹	3052 cm ⁻¹	3087 cm ⁻¹	3107 cm ⁻¹	3243 cm ⁻¹	3248 cm ⁻¹	3261 cm ⁻¹	3297 cm ⁻¹	3334 cm ⁻¹	3427 cm ⁻¹
yyx	10363	323849	45682	401615	691233	233683	1529101	4102663	1832871	6080170	1443884	385713
yyz	30035	674196	11096	719221	224213	158657	646145	1087803	85366	388985	369587	282799
xxx	21696	354096	26979	487593	477409	193238	2642507	4051642	3283871	3756253	721788	43857
xxz	62885	737166	6553	873193	154856	131197	1116631	1074275	152946	240310	184754	32155
xzx	73463	53564	34617	61824	20006	97815	301623	681970	27297	479384	80137	11784
xzz	212924	111512	8409	110717	6489	66411	127455	180821	1271	30669	20512	8640
zxx	73463	53564	34618	61824	20006	97815	301624	681968	27283	479390	80135	11785
zxz	212923	111512	8409	110716	6489	66410	127456	180820	1270	30669	20511	8640
zzx	58892	667099	246942	319932	90277	338985	156659	323474	168400	87117	23867	6291
zzz	170692	1388783	59984	572942	29283	230151	66198	85767	7843	5573	6109	4612
xyx	6926	186960	15844	446263	439411	206196	494062	1159240	2153094	2598485	71330	17457
zyx	102284	262208	66733	10725	68866	38084	91760	242967	279349	183880	29497	3148
xyz	20076	389219	3848	799178	142530	139995	208773	307367	100280	166241	18258	12799
zyz	296458	545872	16210	19207	22337	25856	38774	64421	13010	11763	7550	2308

Table S2. Magnitude of second order susceptibility (in the atomic unit, $e^3 a_0^3 / E_h^2$) relevant to *ssp*, *ppp*, and *psp* polarization of cellulose I β anti-parallel. The C-H and O-H normal modes are presented with blue and red, respectively. The rows in gray signify the components contributing to the SFG signal measured with the *ppp* polarization combination.

Anti-parallel	2999 cm ⁻¹	3007 cm ⁻¹	3024 cm ⁻¹	3052 cm ⁻¹	3087 cm ⁻¹	3107 cm ⁻¹	3243 cm ⁻¹	3248 cm ⁻¹	3261 cm ⁻¹	3297 cm ⁻¹	3334 cm ⁻¹	3427 cm ⁻¹
yyx	0	0	0	0	0	0	0	0	0	0	0	0
yyz	30035	674196	11096	719221	224213	158657	646145	1087803	85366	388985	369587	282799
xxx	0	0	0	0	0	0	0	0	0	0	0	0
xxz	62885	737166	6553	873193	154856	131197	1116631	1074275	152946	240310	184754	32155
xzx	73463	53564	34617	61824	20006	97815	301623	681970	27297	479384	80137	11784
xzz	0	0	0	0	0	0	0	0	0	0	0	0
zxx	73463	53564	34618	61824	20006	97815	301624	681968	27283	479390	80135	11785
zxz	0	0	0	0	0	0	0	0	0	0	0	0
zzx	0	0	0	0	0	0	0	0	0	0	0	0
zzz	170692	1388783	59984	572942	29283	230151	66198	85767	7843	5573	6109	4612
xyx	0	0	0	0	0	0	0	0	0	0	0	0
zyx	102284	262208	66733	10725	68866	38084	91760	242967	279349	183880	29497	3148
xyz	20076	389219	3848	799178	142530	139995	208773	307367	100280	166241	18258	12799
zyz	0	0	0	0	0	0	0	0	0	0	0	0

Table S3. Magnitude of second order susceptibility (in the atomic unit, $e^3 a_0^3 / E_h^2$) relevant to *ssp*, *ppp*, and *psp* polarization of cellulose I α parallel. The C-H and O-H normal modes are presented with blue and red, respectively. The rows in gray signify the components contributing to the SFG signal measured with the *ppp* polarization combination.

Parallel	2963 cm ⁻¹	2974 cm ⁻¹	2982 cm ⁻¹	2994 cm ⁻¹	3015 cm ⁻¹	3029 cm ⁻¹	3333 cm ⁻¹	3346 cm ⁻¹	3380 cm ⁻¹	3402 cm ⁻¹	3416 cm ⁻¹	3435 cm ⁻¹
yx	24755	53143	20102	33270	32998	496106	2055931	2085768	3255837	5423466	3320020	4908981
yyz	447422	307027	295463	263186	587054	430797	113252	20507	264846	386269	175204	19719
xxx	17974	55595	8112	29102	17338	612666	3287574	2989481	3552830	4519411	140407	199067
xxz	324861	321194	119240	230221	308456	532013	181099	29393	289005	321881	7409	799
xzx	14651	66174	7388	33218	27553	136255	105897	109889	213443	274486	28622	49343
xzz	264798	382313	108590	262780	490183	118318	5833	1080	17362	19549	1510	198
zxx	14651	66174	7388	33218	27553	136252	105906	109894	213438	274505	28630	49335
zxz	264800	382315	108589	262780	490185	118316	5833	1080	17362	19550	1510	198
zxx	77709	212602	67573	136049	72852	630579	91780	177938	308639	474831	136955	61980
zzz	1404474	1228282	993207	1076228	1296077	547568	5055	1749	25106	33818	7227	248
xyx	3390	2792	1473	14106	115	426000	1000490	808923	1610091	1271448	169383	499836
zyx	16281	12802	14210	15058	23813	202870	112675	204109	174129	12452	275715	120592
xyz	61278	16130	21658	111593	2054	369920	55112	7953	130972	90555	8938	2007
zyz	294262	73963	208869	119119	423655	176164	6206	2006	14164	886	14550	484

Table S4. Magnitude of second order susceptibility (in the atomic unit, $e^3 a_0^3 / E_h^2$) relevant to *ssp*, *ppp*, and *psp* polarization of cellulose I α anti- parallel. The C-H and O-H normal modes are presented with blue and red, respectively. The rows in gray signify the components contributing to the SFG signal measured with the *ppp* polarization combination.

Anti-parallel	2963 cm ⁻¹	2974 cm ⁻¹	2982 cm ⁻¹	2994 cm ⁻¹	3015 cm ⁻¹	3029 cm ⁻¹	3333 cm ⁻¹	3346 cm ⁻¹	3380 cm ⁻¹	3402 cm ⁻¹	3416 cm ⁻¹	3435 cm ⁻¹
yyx	0	0	0	0	0	0	0	0	0	0	0	0
yyz	447422	307027	295463	263186	587054	430797	113252	20507	264846	386269	175204	19719
xxx	0	0	0	0	0	0	0	0	0	0	0	0
xxz	324861	321194	119240	230221	308456	532013	181099	29393	289005	321881	7409	799
xzx	14651	66174	7388	33218	27553	136255	105897	109889	213443	274486	28622	49343
xzz	0	0	0	0	0	0	0	0	0	0	0	0
zxx	14651	66174	7388	33218	27553	136252	105906	109894	213438	274505	28630	49335
zxz	0	0	0	0	0	0	0	0	0	0	0	0
zzx	0	0	0	0	0	0	0	0	0	0	0	0
zzz	1404474	1228282	993207	1076228	1296077	547568	5055	1749	25106	33818	7227	248
xyx	0	0	0	0	0	0	0	0	0	0	0	0
zyx	16281	12802	14210	15058	23813	202870	112675	204109	174129	12452	275715	120592
xyz	61278	16130	21658	111593	2054	369920	55112	7953	130972	90555	8938	2007
zyz	0	0	0	0	0	0	0	0	0	0	0	0

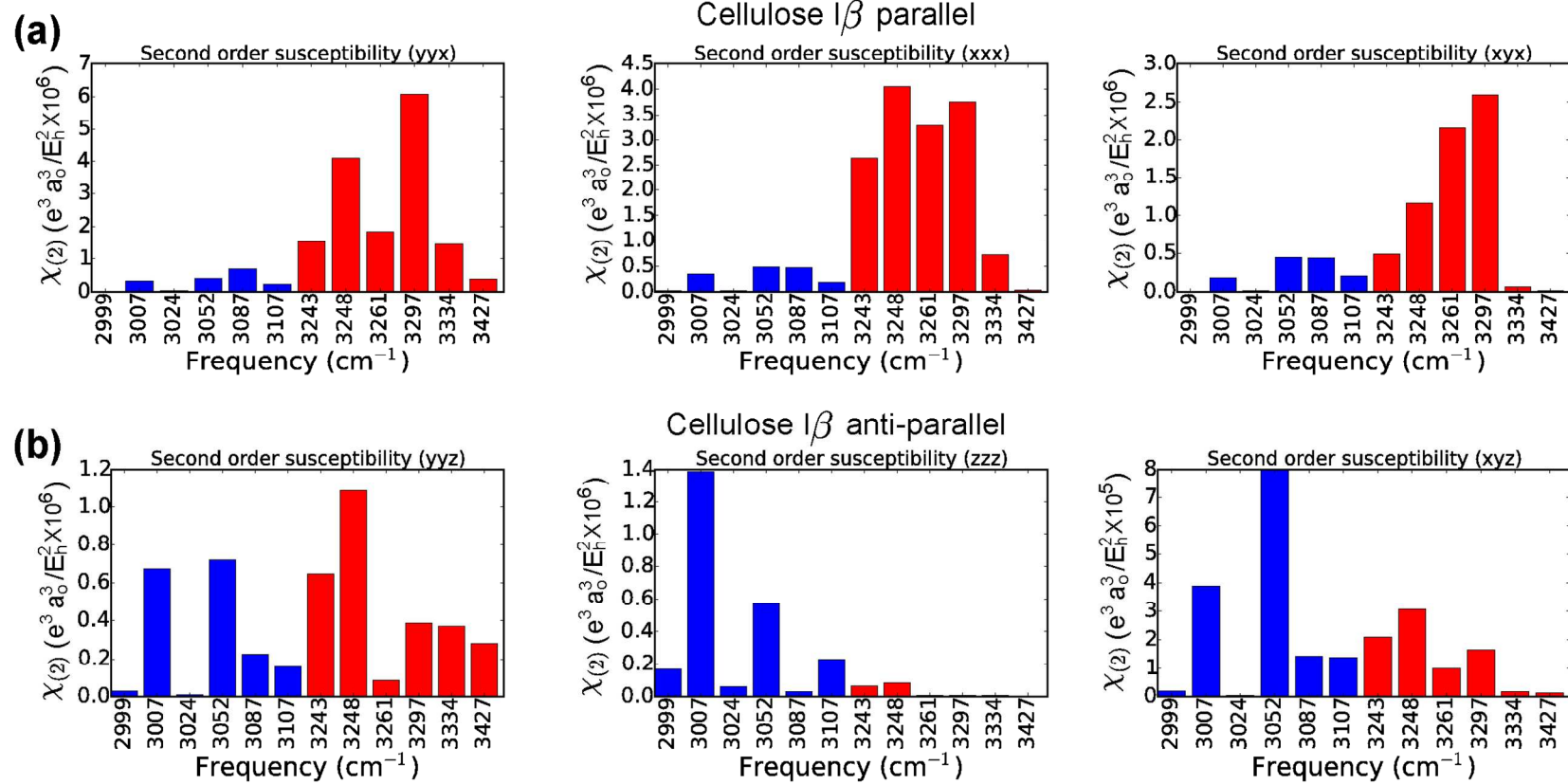


Figure S3. The dominant components in second order susceptibility for the selected normal modes in cellulose I β , (a) parallel and (b) anti-parallel. The C-H and O-H normal modes are color coded by blue and red, respectively.

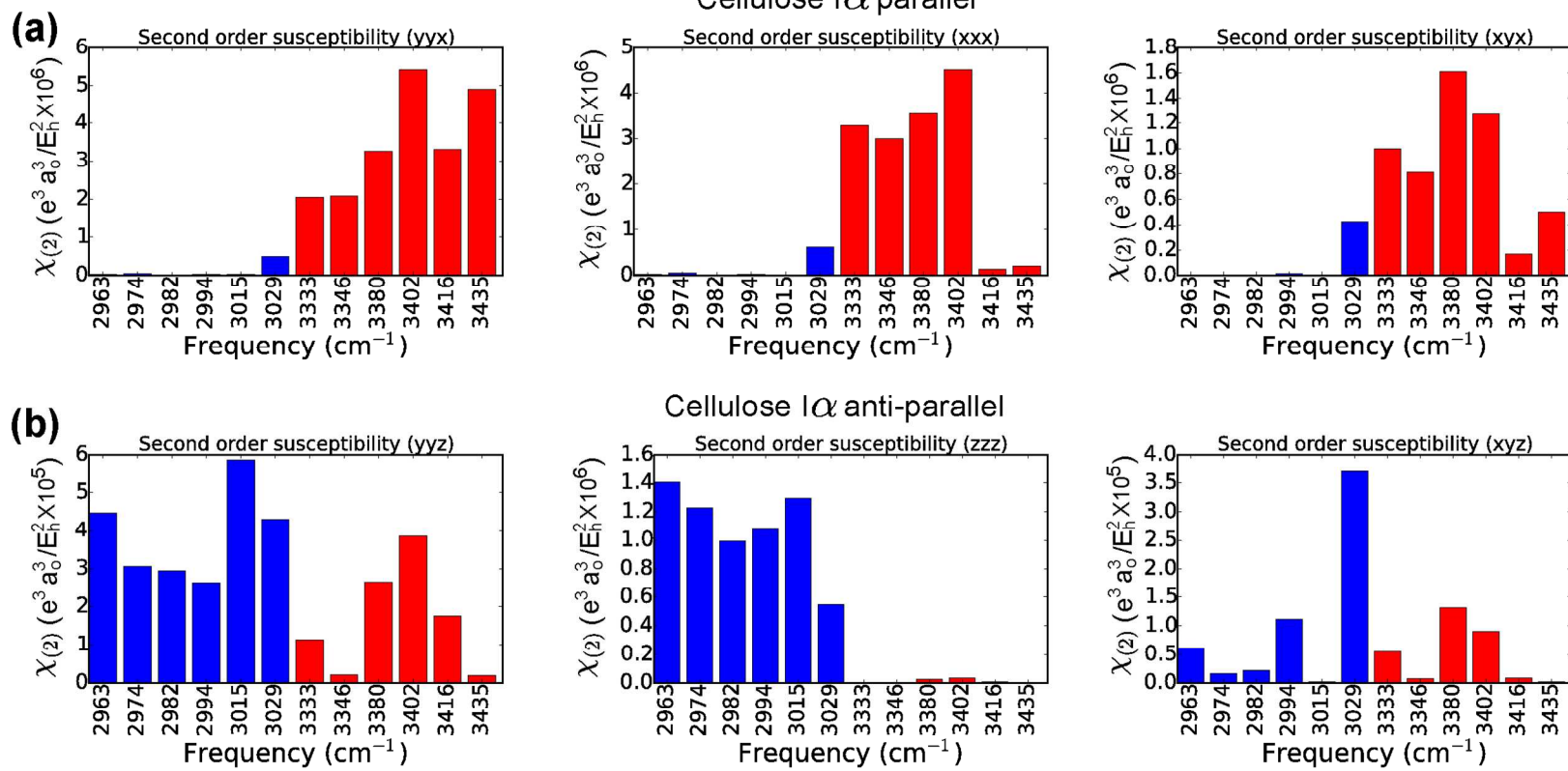


Figure S4. The dominant components in second order susceptibility for the selected normal modes in cellulose I α , (a) parallel and (b) anti-parallel. The C-H and O-H normal modes are color coded by blue and red, respectively.

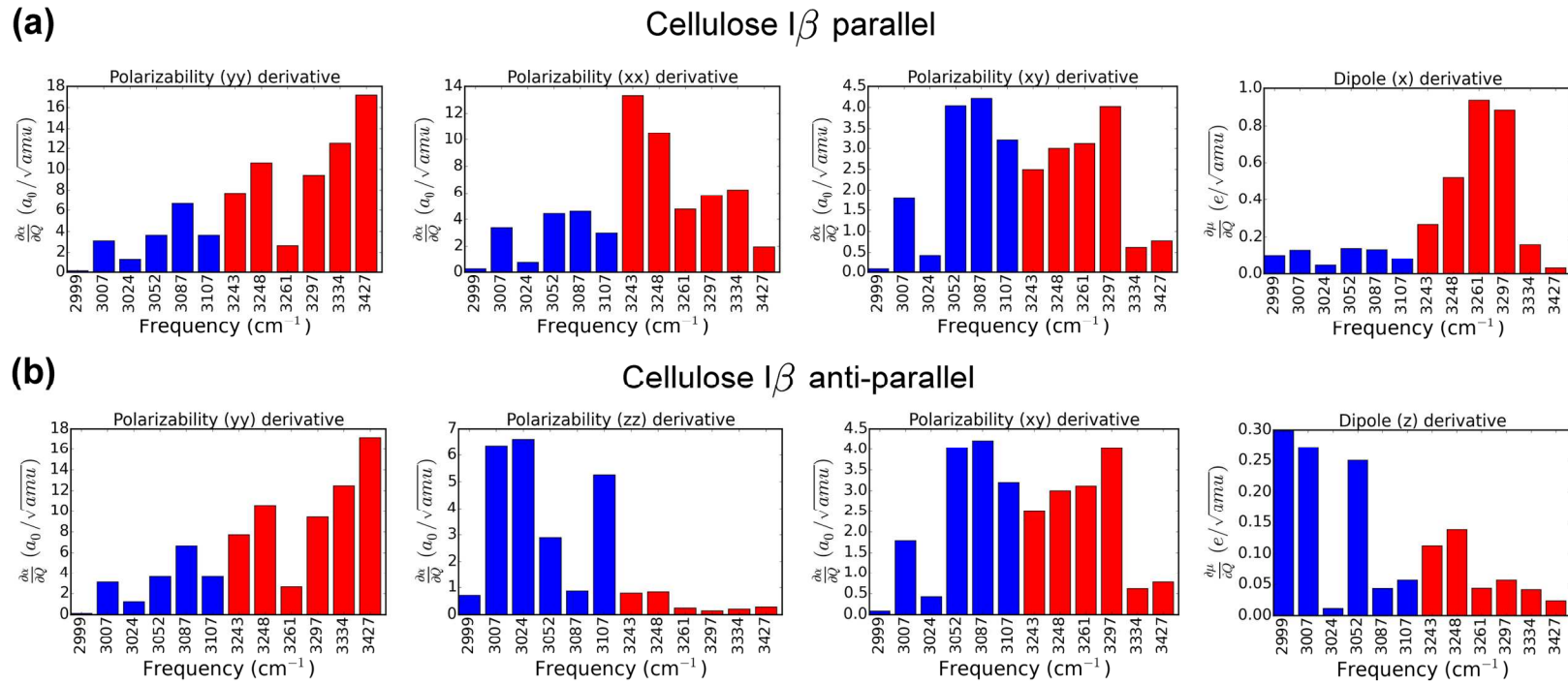


Figure S5. The dominant components of the derivatives of polarizability and dipole for the selected normal modes in cellulose I β , (a) parallel and (b) anti-parallel. The C-H and O-H normal modes are color coded by blue and red, respectively. In (b) the dipole derivative along the x and y directions are zero, so the dipole derivative along the z-direction is dominant.

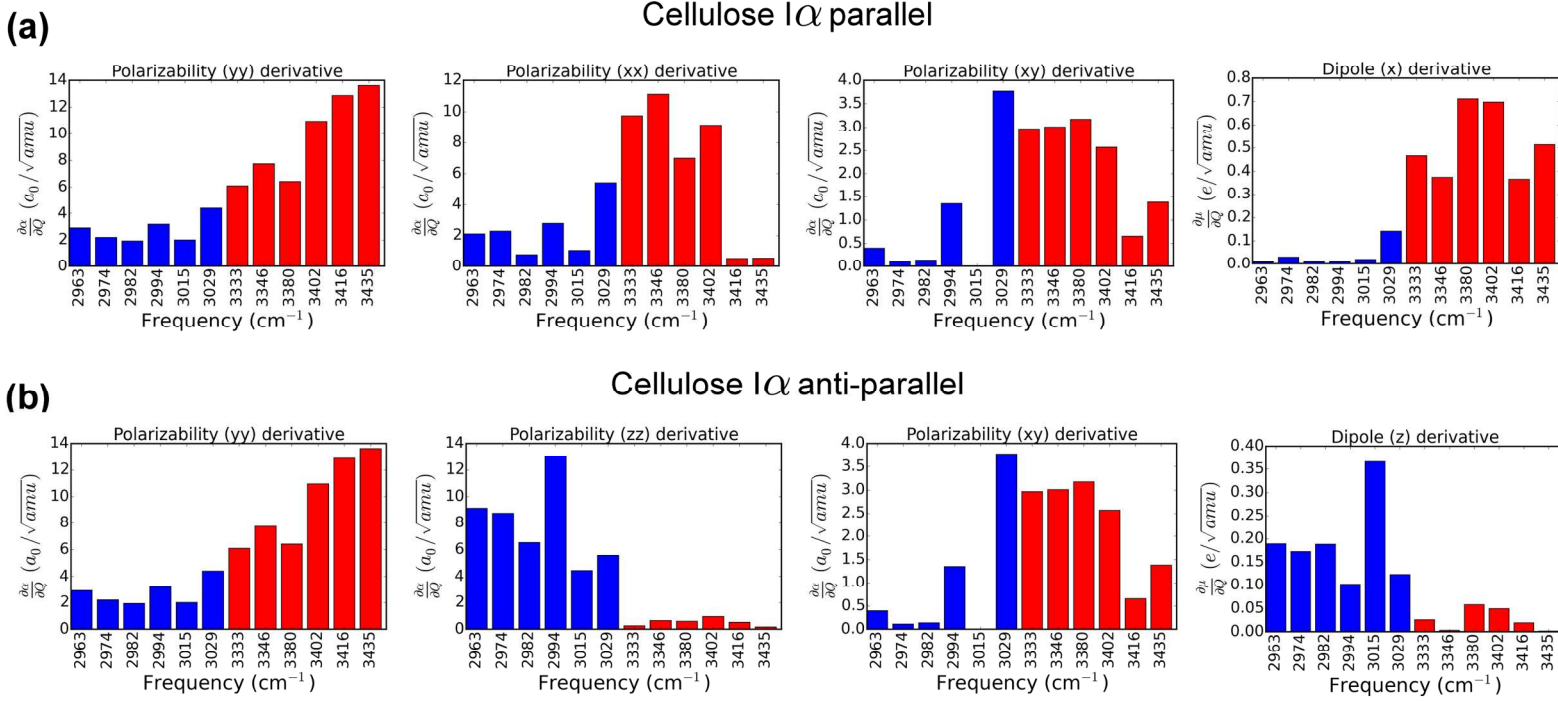


Figure S6. The dominant components of the polarizability and dipole for the selected normal modes in cellulose I α , (a) parallel and (b) anti-parallel. The C-H and O-H normal modes are color coded by blue and red, respectively. In (b) the polarizability and dipole derivative along the x and y directions are zero, so the dipole derivative along the z-direction is dominant.

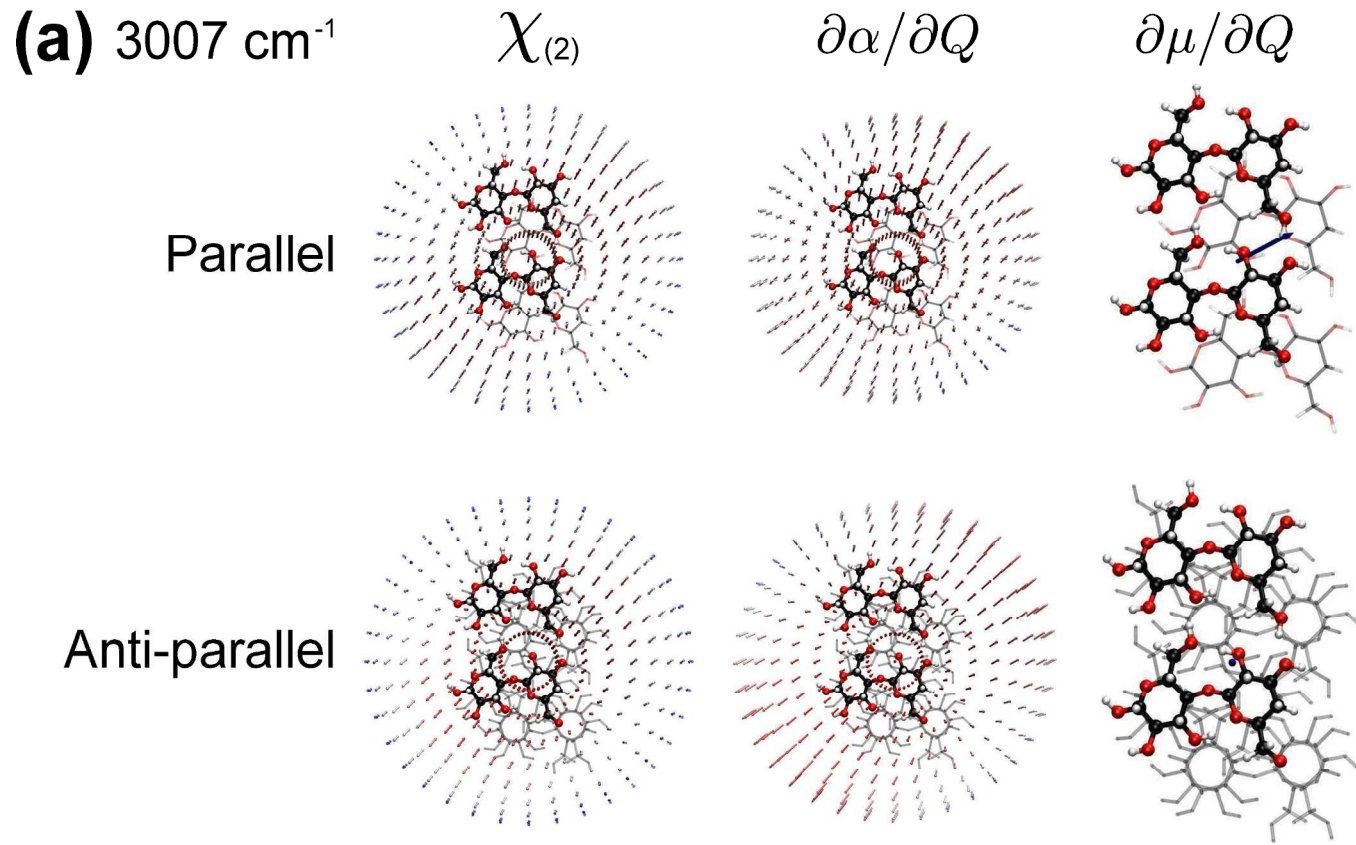
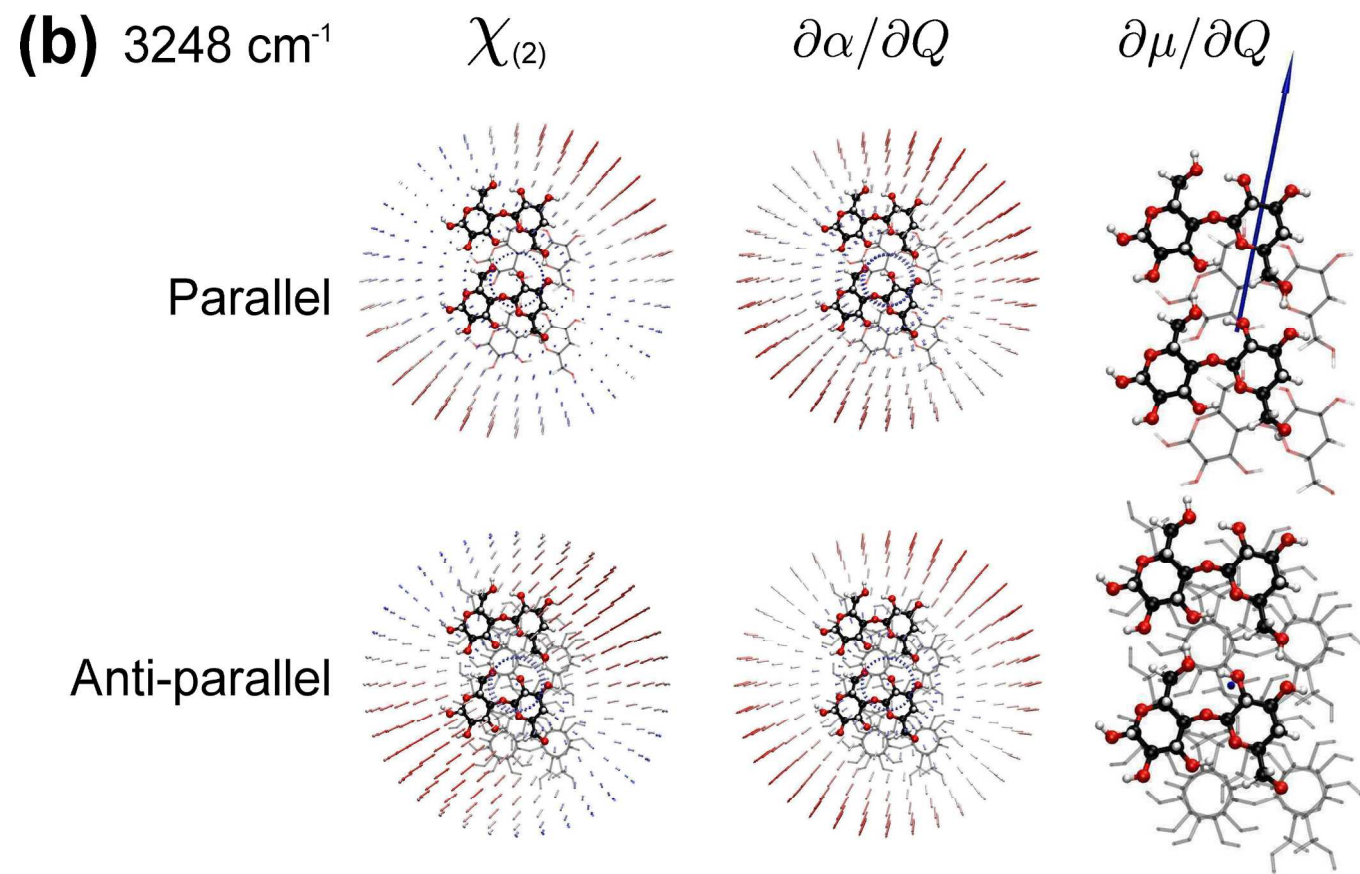


Figure S7. Graphical presentations of the second-order susceptibility tensor $(\chi_{XYZ}^{(2)})$ and derivatives of the polarizability matrix and dipole moment vector for cellulose I β (a-c) and I α (d-f). Unit sphere representation of second susceptibility and polarizability do not change dramatically in parallel and anti-parallel cellulose. The dipole vectors are significantly modified from parallel to anti-parallel, particularly for the OH normal modes, shown in the blue arrows.



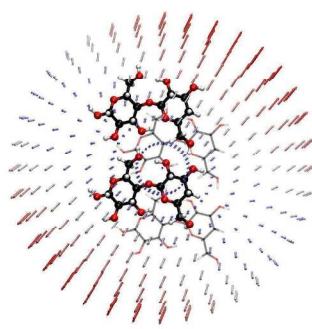
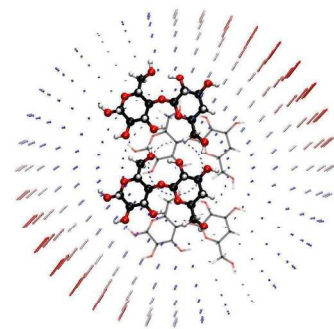
(c) 3297 cm^{-1}

$\chi_{(2)}$

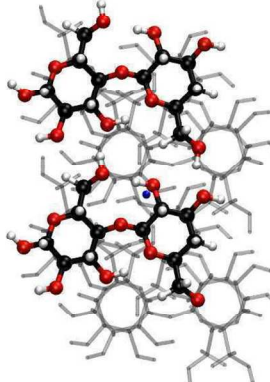
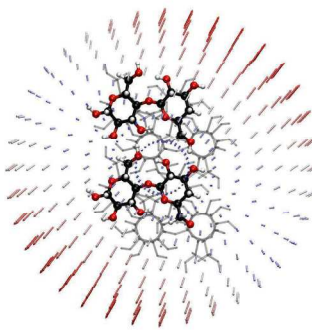
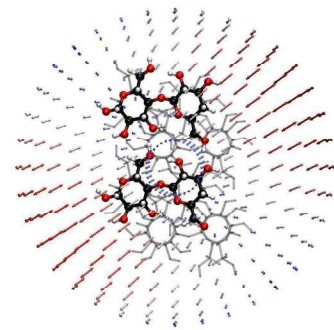
$\partial\alpha/\partial Q$

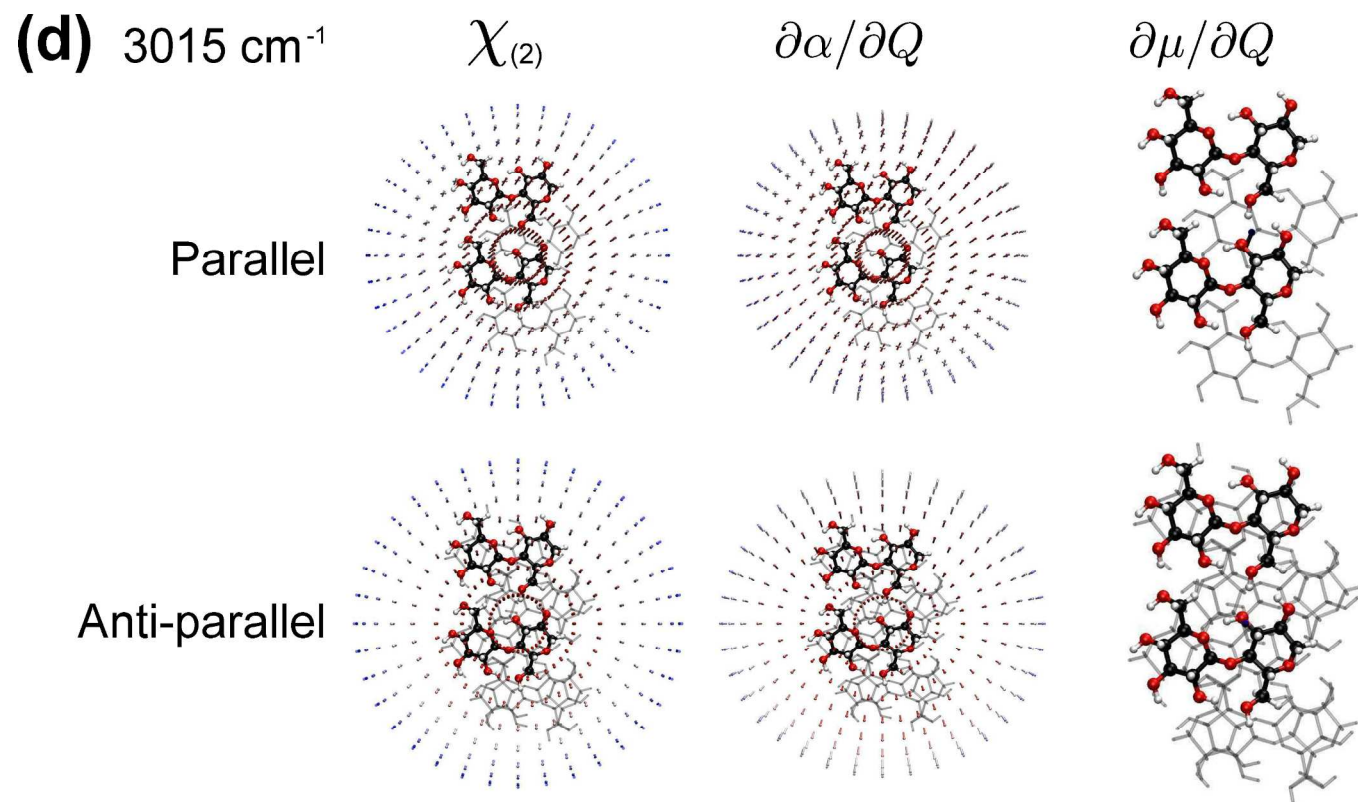
$\partial\mu/\partial Q$

Parallel



Anti-parallel





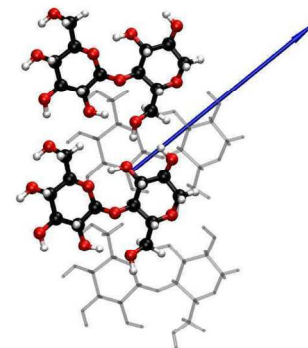
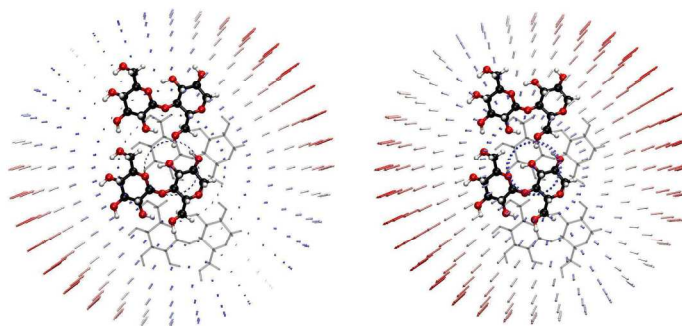
(e) 3333 cm^{-1}

$\chi_{(2)}$

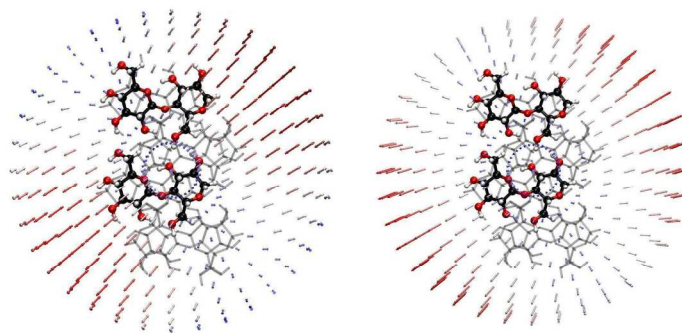
$\partial\alpha/\partial Q$

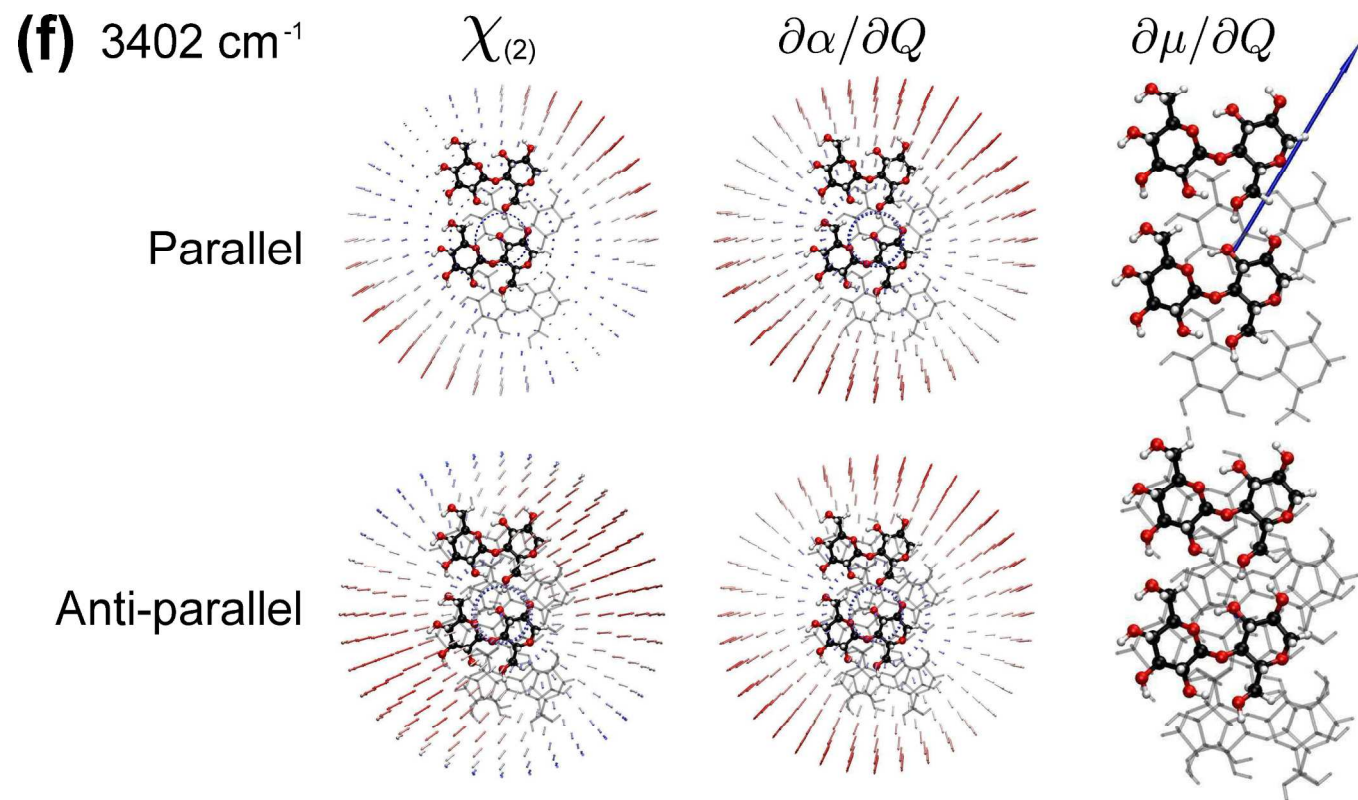
$\partial\mu/\partial Q$

Parallel



Anti-parallel





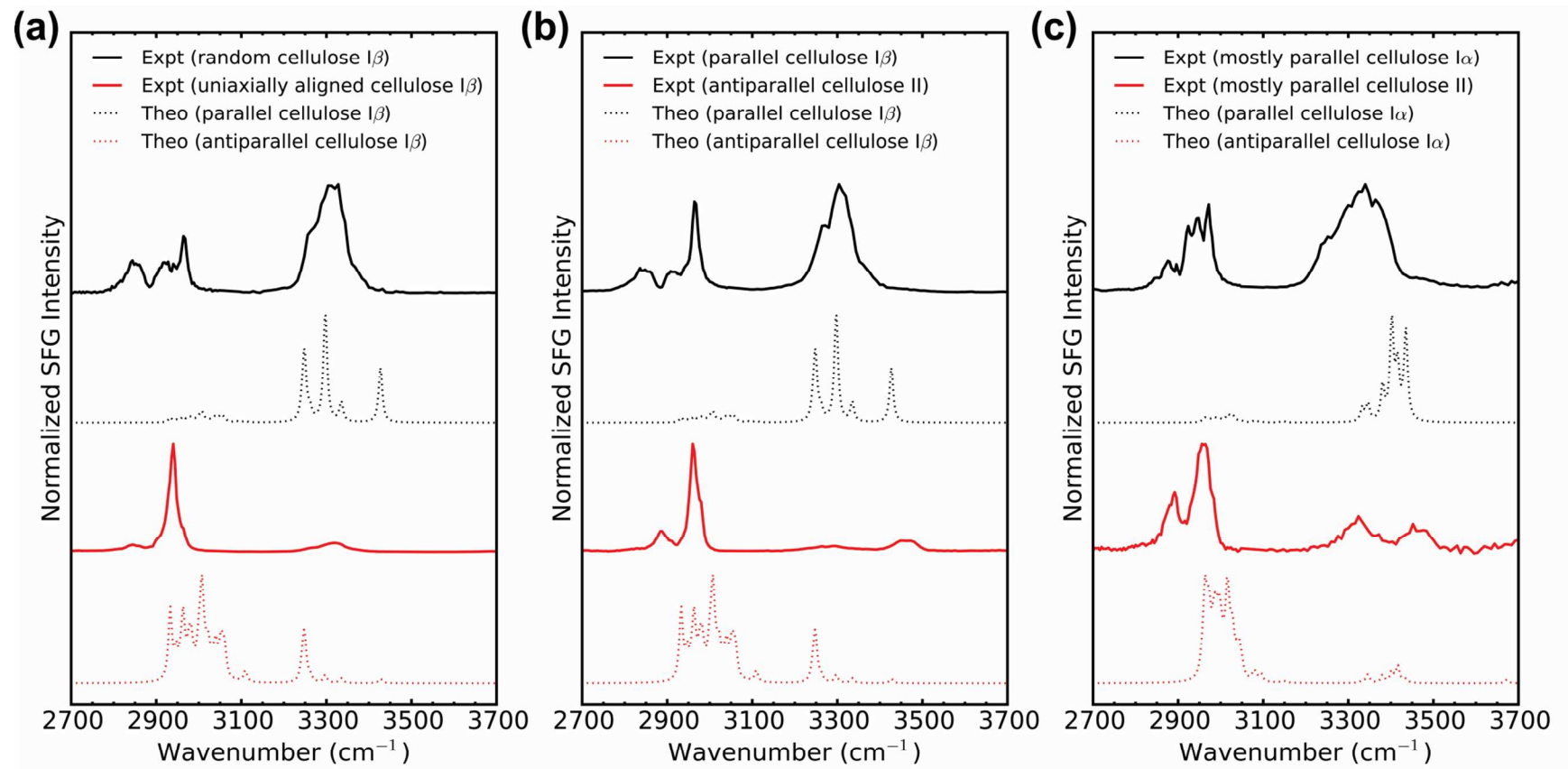


Figure S8. Comparison of the relative intensities of the simulated spectra (Figure 2) and the experimental spectra (Figure 4).

Table S5. List of all *unscaled* OH, CH, CH₂ (s; symmetric) and CH₂ (as; asymmetric) vibrational frequencies from TD-DFT calculations for the truncated cellulose I β model. For most frequencies, the vibrational motion is not localized to one functional group, but de-localized through the entire crystal. Therefore, the predominant vibration is labelled (primary) and minor vibrations (secondary). The unique OH peak characteristic of cellulose I β is shown in gray in the experimental data column. The peak assignment was reported in our previous papers comparing the experimental data with DFT calculations with periodic boundary conditions for the full crystal lattice.

Vibration mode assignment (TD-DFT)		frequency (cm ⁻¹)	Vibration mode assignment (TD-DFT)		frequency (cm ⁻¹)	Vibration mode assignment (experimental)	frequency (cm ⁻¹)	Reference	
primary	secondary		primary	secondary					
3OH	--	3541	1,2,3,4,5CH	CH2 s	3024	weakly hydrogen bonded OH groups in less-crystalline regions	3450 (broad)	Lee et al. (2015) ³	
6OH	--	3497	CH2 as	1,2,3,4,5CH	3022				
6OH	--	3491	CH2 s	1,2,3,4,5CH	3016				
2OH	--	3472	CH2 as	1,2,3,4,5CH	3013				
2OH	--	3472	CH2 s	1,2,3,4,5CH	3009				
3OH	--	3446	CH2 s	1,2,3,4,5CH	3009				
6OH	2OH, 3OH	3427	CH2 s	1,2,3,4,5CH	3007		2,3,6OH 3270		
6OH	2OH, 3OH	3335	CH2 s	1,2,3,4,5CH	3006				
3OH	2OH, 6OH	3297	CH2 as	1,2,3,4,5CH	3006				
3OH	2OH, 6OH	3262	1,2,3,4,5CH	CH2 s	3004		2968	Lee et al. (2013) ⁴	
2OH	3OH, 6OH	3248	1,2,3,4,5CH	CH2 s	3004		2944		
2OH	3OH, 6OH	3243	CH2 as	1,2,3,4,5CH	3000		2920		
CH2 as	5CH	3110	CH2 s	1,2,3,4,5CH	2999		2886		
CH2 as	5CH	3107	CH2 s	1,2,3,4,5CH	2998		2850		
CH2 as	5CH, CH2 s	3088	1,2,3,4,5CH	CH2 s	2994				
CH2 as	5CH, CH2 s	3064	1,2,3,4,5CH	CH2 s	2990				

CH2 as	5CH, CH2 s	3060	CH2 s	1,2,3,4,5CH	2989
CH2 s	5CH	3055	CH2 s	1,2,3,4,5CH	2983
CH2 s	5CH	3054	CH2 s	1,2,3,4,5CH	2981
CH2 s	5CH	3054	CH2 s	1,2,3,4,5CH	2979
CH2 as	5CH	3052	1,2,3,4,5CH	CH2 s	2978
CH2 s	5CH	3051	CH2 s	1,2,3,4,5CH	2976
CH2 s	5CH	3050	1,2,3,4,5CH	CH2 s	2976
CH2 s	1,2,3,4,5CH	3042	CH2 s	1,2,3,4,5CH	2974
CH2 s + CH	1,2,3,4,5CH	3039	CH2 s	1,2,3,4,5CH	2972
CH2 as	1,2,3,4,5CH	3038	CH2 s	1,2,3,4,5CH	2963
1,2,3,4,5CH	CH2 s	3034	1,2,3,4,5CH	CH2 s	2960
1,2,3,4,5CH	CH2 s	3033	CH2 s	1,2,3,4,5CH	2957
1,2,3,4,5CH	CH2 s	3030	CH2 s	1,2,3,4,5CH	2947

Table S6. List of all *unscaled* OH, CH, CH₂ (s; symmetric) and CH₂ (as; asymmetric) vibrational frequencies from TD-DFT calculations for the truncated cellulose Iα model. For most frequencies, the vibrational motion is not localized to one functional group, but de-localized through the entire crystal. Therefore, the predominant vibration is labelled (primary) and minor vibrations (secondary). The unique OH peak characteristic of cellulose Iα is shown in gray in the experimental data column. The peak assignment was reported in our previous papers comparing the experimental data with DFT calculations with periodic boundary conditions for the full crystal lattice.

Vibration mode assignment (TD-DFT)		frequency (cm ⁻¹)	Vibration mode assignment (TD-DFT)		frequency (cm ⁻¹)	Vibration mode assignment (experimental)	frequency (cm ⁻¹)	Reference
primary	secondary		primary	secondary				
6OH	2OH	3435	1,2,3,4,5CH	CH2 s	2996	weakly hydrogen bonded OH groups in less-crystalline regions	3450 (broad)	Lee et al. (2015) ³
6OH	2OH,3OH	3429	CH2 as	1,2,3,4,5CH	2995			
6OH	2OH,3OH	3416	1,2,3,4,5CH	CH2 s	2994			
6OH	2OH,3OH	3412	CH2 s	1,2,3,4,5CH	2990			
2OH	6OH,3OH	3402	CH2 s	1,2,3,4,5CH	2989			
2OH	6OH,3OH	3380	1,2,3,4,5CH	CH2 as	2988			
3OH	6OH, 2OH	3346	1,2,3,4,5CH	CH2 s	2987			
3OH	6OH, 2OH	3333	1,2,3,4,5CH	CH2 s	2987			
CH2 as	5CH	3148	1,2,3,4,5CH	CH2 s	2987	2OH	3240	Lee et al. (2013) ⁴
CH2 as	5CH	3142	1,2,3,4,5CH	CH2 s	2986	CH2 as	2968	
CH2 as	5CH, CH2 s	3083	1,2,3,4,5CH	CH2 s	2985	CH2 as	2944	
CH2 as	5CH, CH2 s	3080	1,2,3,4,5CH	CH2 s	2985	CH2 as	2920	
CH2 as	5CH, CH2 s	3078	CH2 s	1,2,3,4,5CH	2982	CH2 s	2886	
CH2 s	5CH	3050	1,2,3,4,5CH	CH2 as	2977	CH2 s	2850	
CH2 s	5CH	3044	CH2 s	1,2,3,4,5CH	2974			

CH2 s	5CH	3039	CH2 s	1,2,3,4,5CH	2970
CH2 as	5CH	3038	CH2 s	1,2,3,4,5CH	2969
CH2 as	5CH	3030	CH2 s	1,2,3,4,5CH	2963
CH2 as	5CH	3029	1,2,3,4,5CH	--	2963
1,2,3,4,5CH	CH2 s	3026	1,2,3,4,5CH	CH2 as	2962
1,2,3,4,5CH	CH2 as	3022	1,2,3,4,5CH	CH2 s	2956
CH2 s	--	3018			
1,2,3,4,5CH	CH2 s	3015			
1,2,3,4,5CH	CH2 s	3011			
1,2,3,4,5CH	CH2 as	3008			
1,2,3,4,5CH	CH2 s	3007			
1,2,3,4,5CH	CH2 s	3003			
1,2,3,4,5CH	--	3001			
CH2 s	1,2,3,4,5CH	2999			

References

1. Bennett, D.W. *Understanding single-crystal x-ray crystallography*; John Wiley & Sons, 2010.
2. Wang, H.-F.; Velarde, L.; Gan, W.; Fu, L. Quantitative Sum-Frequency Generation Vibrational Spectroscopy of Molecular Surfaces and Interfaces: Lineshape, Polarization, and Orientation. *Annu. Rev. Phys. Chem.* **2015**, *66*, 189-216.
3. Lee, C. M.; Kubicki, J. D.; Xin, B.; Zhong, L.; Jarvis, M. C.; Kim, S. H. Hydrogen Bonding Network and OH Stretch Vibration of Cellulose: Comparison of Computational Modeling with Polarized IR and SFG spectra. *J. Phys. Chem. B* **2015**, *119*, 15138–15149.
4. Lee, C. M.; Mohamed, N. M. A.; Watts, H. D.; Kubicki, J. D.; Kim, S. H. Sum-Frequency-Generation (SFG) Vibration Spectra and Density Functional Theory Calculations with Dispersion Corrections (DFT-D2) for Cellulose I α and I β . *J. Phys. Chem. B* **2013**, *117*, 6681–6692.